CHEMIJA. 2017. Vol. 28. No. 4. P. 214–225

Modification of polyamide films by semiconductive and conductive copper selenide–copper sulfide layers

Vitalijus Janickis,

Neringa Petrašauskienė*

Kaunas University of Technology,
Radvilėnų Rd. 19,
50254 Kaunas, Lithuania

Modification of the surface of polyamide 6 (PA) films by semiconductive and electrically conductive layers of mixed copper selenide–copper sulfide, Cu_xSe–Cu_yS, was performed using the sorption–diffusion method and the water solutions of potassium selenopentathionate, $K_2SeS_4O_6$, as the precursor of polymer chalcogeniumization. Selenopentathionate anions containing divalent selenium and sulfur atoms of low oxidation state, ^-O_3S-S-Se-S-SO_3^-, are sorbed-diffused into PA films if they are treated with selenopentathionate solutions. Cu_xSe–Cu_yS layers form on the surface of a PA (polyamide 6) film when a chalcogeniumized polymer is treated with a water solution of copper(II/I) salt: the anions of selenopentathionate react with copper ions. The concentration of sulfur, selenium and copper increases with an increase of the concentration and temperature of a precursor solution and the duration of PA initial chalcogeniumization. The formed layers were characterized for chemical composition, electrical and physical properties. The percentage amounts of selenium, sulfur and copper in Cu_xSe–Cu_yS layers on PA films increase with polymer chalcogeniumization time. The X–ray diffraction (XRD) pattern study of Cu_xSe–Cu_yS layers showed that they are polycrystalline in nature. The six phases of copper selenides – Cu_2Se, $CuSe_2$, $CuSe_2$, Cu_3Se_2, berzellianite $Cu_{2-x}Se$ and bellidoite Cu_2Se, also the four phases of copper sulfides – monoclinic djurleite, $Cu_{1.9375}Se$, cubic digenite, $Cu_{1.8}S$, orthorhombic chalcocite, Cu_2S, and orthohrombic anilite, $Cu_{1.75}S$, have been identified. With an increase of the concentration and temperature of the precursor solution and the duration of PA treatment the highest concentration of conductive copper selenides is reached and the composition of Cu_xSe phases changes in the direction of a decrease of *x*. XPS results confirmed the formation of copper selenides–copper sulfides layers on the surface of PA. The regularities established enable formation of Cu_xSe–Cu_yS layers of the desirable composition and conductivity. Studies by the method of atomic force microscopy (AFM) showed that depending on the conditions (duration of chalcogeniumization, concentration and temperature) of the PA initial treatment in the $K_2SeS_4O_6$ solution (under the same "copperizing" conditions), the formation of copper chalcogenide layers proceeds irregularly in the form of islands which grow into larger agglomerates. The surface of the layer is uneven, rather rough.

Keywords: polyamide, copper selenide–copper sulfide layer, scanning electron microscopy, X-ray diffraction, X-ray photoelectron spectroscopy, atomic force microscopy

*Corresponding author. Email: neringa.petrasauskiene@ktu.lt

INTRODUCTION

Copper chalcogenides Cu_xY (Y = S, Se, Te) and thin layers of Cu_xY, owing to their variations in stoichiometric composition, nanocrystal morphology, complex structure, valence states and other unique properties, have potential applications in numerous fields [1–7]: they are semiconductors with thermoelectric properties, ionic conductivity and therefore found applications in various devices, for example, as solar cells, optical data storage [8–10], super ionic conductors, photo-detectors, photothermal converters, electroconductive electrodes, microwave shielding coating, gas sensors, etc. [11–27].

The methods of vacuum evaporation, activated reactive evaporation, spray pyrolysis, electroless deposition, successive ionic layer adsorption and reaction (SILAR), and chemical bath deposition [28–36] have been used for the formation of copper chalcogenides layers on various dielectrics as well as on polymers.

Over the last decade, a sorption–diffusion method for the formation of copper chalcogenide layers on the surface of polyamide based on the initial treatment of a polymer with the solutions containing anions of polythionic compounds has been under extensive investigation in our laboratory [22–23, 26–27, 30, 37–82]. The polythionic compound anions, containing chains of divalent chalcogens atoms of a low oxidation state [78–79, 83] (the polythionates, $^-O_3S–S_x–SO_3^-$, selenopolythionates, $^-O_3S–SeS_x–SO_3^-$, among them – selenopentathionate, $^-O_3S–S–Se–S–SO_3^-$), are sorbed by a polymer. After chalcogeniumized PA being treated with a solution of copper(II/I) salt, layers of various copper chalcogenides, for example, sulfides, Cu_xS [22, 38, 42–59], selenides, Cu_xSe [23, 60–64], mixed copper selenide–copper sulfide, $Cu_xSe–Cu_yS$ [26, 65–68, 70–71, 74–77, 80], or mixed copper selenide–copper telluride, $Cu_xSe–Cu_yTe$ [27, 69, 72–73], on the surface of a polymer were formed.

The aim of the present work was to summarize and to discuss the results obtained by us studying the formation and characterization of mixed copper selenide–copper sulfide layers on PA films by the sorption–diffusion method, since mainly only separate fragments of these studies in our previous publications have been described [26, 65–68, 70–71, 74–77, 80].

EXPERIMENTAL

The modification of a PA film by the formation of mixed copper chalcogenides layers on its surface was performed in two stages. In the first stage, the PA film was treated in solutions of potassium selenopentathionate. In the second stage, the chalcogeniumized PA films were treated with a water solution of copper salt: the interaction of copper ions with the sulfur and selenium atoms of a low oxidation state present in the sorbed selenopentathionate ions leads to the formation of mixed copper chalcogenides layers of various chemical, phase composition and electrical conductance.

The layers of copper chalcogenides were deposited on the PA film (specification TY 6-05-1775-76) of 70 μm thickness produced in Russia. The samples of 15 × 70 mm in size were used. Before the chalcogeniumization, they were boiled in distilled water for 2 h to remove the remainder of the monomer. Then they were dried using filter paper and then over $CaCl_2$ for 24 h. Distilled water, reagents of the grades "especially pure", "chemically pure" and "analytically pure" were used in the experiments.

The samples of the PA film were chalcogenized in 0.025, 0.05, 0.1 and 0.2 mol/dm^3 solutions of $K_2SeS_4O_6$ in 0.1 mol/dm^3 HCl (pH ~ 1.5) at 30 and 50°C. For the formation of mixed $Cu_xSe–Cu_yS$ layers the samples of chalcogeniumized PA were treated with a Cu(II/I) salt solution at 78°C. The Cu(II/I) salt solution was made from crystalline $CuSO_4 \cdot 5H_2O$ and a reducing agent hydroquinone 84, 85]. It is a mixture of univalent and divalent copper salts, in which there are 0.34 mol/dm^3 of Cu(II) salt and 0.06 mol/dm^3 of Cu(I) salt [85]. After having been kept in the $K_2SeS_4O_6$ solution, the sample was treated with a Cu(II/I) solution, then rinsed with distilled water, dried over $CaCl_2$ and used in consequent experiments.

The salt of potassium selenopentathionate, $K_2SeS_4O_6 \cdot 1.5H_2O$, was prepared and analysed according to published procedures [86]. It was stored in darkness at the temperature of – 5°C (in a freezer).

The concentrations of selenium and copper in the modified PA film samples were determined using an atomic absorption spectrometer Perkin–Elmer 503 (λ = 196 nm for selenium and λ = 324.8 nm for copper) [87].

Before the analysis, samples of PA strips containing $Cu_xSe–Cu_yS$ layers had to be mineralized. The samples were treated with concentrated HNO_3 to destroy PA and to oxidize selenium and sulfur compounds to selenite and sulfate. Heating with concentrated hydrochloric acid removed the excess of nitric acid. The sulfur compounds in PA strips in the form of sulfate were determined turbidimetrically [88].

The phase composition of copper chalcogenide layers on the surface of PA was investigated by means of X-ray diffraction with a DRON-6 diffractometer provided with a special device for beam limitation at low and medium diffraction angles using graphite-monochromatized Cu-K_α radiation source (λ = 1.54178 Å) under a voltage of 30 kV and a current of 30 mA. The XRD patterns were recorded with a step size of 0.05° from 2θ = 30° to 70°. X-ray diffractograms of the PA samples with the layers of copper chalcogenides were treated using the program Search Match to eliminate the maxima of PA.

Microscopic studies of the $Cu_xSe–Cu_yS$ layers were performed using scaning electronic microscope JEOL SM-IC25S.

The UV,VIS (200–450 nm) and IR (400–1400 cm^{-1}) spectra were obtained by spectrometers Spectronic^{R} Genesys^{TM} and Perkin-Elmer GX system FT-IR.

The XPS technique was used to determine the chemical composition of the layers. XPS measurements were performed by a Kratos Analytical AMICUS/ESCA 3400 analyser (Mg K_α radiation, 240 W). Scan photoelectron spectra were recorded for Cu 2*p*, S 2*p*, Se 3*d* and O 1*s*. The photoelectron peaks were calibrated against the carbon line C 1*s* with a binding energy equal to 285 eV. Empirical sensitivity factors for these elements were taken from the literature [89] and the spectra obtained were compared with the standard ones [90].

The electrical sheet resistance at a constant current of $Cu_xSe–Cu_yS$ layers was measured using a 4–point probe technique.

The morphology of the surface of $Cu_xSe–Cu_yS$ layers, the quantitative microscopy of the roughness of layers formed on the PA surface were studied with a NT-206 atomic force microscope, in the contact regime with high resolution probes with the force constant k = 3 N/m. The characteristics of the atomic force microscope are the following: the maximum scan field area 10 × 10 to 30 × 30 microns, the measurement matrix up to 512 × 512 points and more, the maximum range of measured heights 4 microns, vertical resolution 0.1–0.2 nm. The AFM cantilever was produced by Silicon-MDT in cooperation with MikroMasch (Estonia): NONCONTACT silicon cantilever NSC11/15 type; characteristics of the cantilever: the radius of the curvature less than 10 nm; the tip height 15–20 μm, the full tip cone angle less than 20°. Lateral force microscopy studies are useful for imaging variations in surface friction that can arise from inhomogeneities in the surface material, and also for obtaining edge-enhanced images. The data of measurements were analysed using the Surface View 2.0 program.

RESULTS AND DISCUSSION

The preparation of semiconducting and conductive layers of copper selenides–copper sulfides, $Cu_xSe–Cu_yS$, by sorption–diffusion on the surface of PA

For investigation of selenium and sulfur containing particles sorption on and diffusion into PA from potassium selenopentathionate solutions it was indispensable to ascertain in what form (as elemental selenium, sulfur, its radicals or selenopentathionate ions, $SeS_4O_6^{2-}$) selenium and sulfur adsorb PA.

Our investigations showed that the semi-hydrophilic PA adsorbs selenopentathionate ions from these solutions. The sorption of selenopentathionate ions by PA has been studied by IR and UV absorption spectroscopies [77]. The peaks in the IR spectra were found in the intervals 449–460, 534–535, 608, 1017 and 1223–1226 cm^{-1} and have been assigned to the ν(S–S), δ_{as}(O–S–O), δ_s(O–S–O), ν_s(S–O) and ν_{as}(S–O), respectively. The data confirmed that the ions of selenopentathionate are sorbed into PA, because of similarity of the peaks of the former with the peaks in the IR spectra of $K_2SeS_4O_6$, respectively, at 421–452, 536, 618–637, 1027–1036, 1226 cm^{-1}.

The three absorption maxima were observed in the UV absorption spectra: at 240–250 nm, at 280 nm and at 280–320 nm as a clear shoulder. The UV absorption spectra of chalcogeniumized PA are analogous to the UV spectrum of $K_2SeS_4O_6$ solution but all peaks in the chalcogeniumized polymer spectra are moved towards lower frequencies because of sorbed selenopentathionate bonds with the chelating groups of a polymer. Thus, the UV and IR absorption spectra confirmed that sulfur and selenium were sorbed into PA in the form of selenopentathionate ions.

The chemical analysis of the chalcogeniumized PA samples showed that the concentration of sulfur and selenium sorbed on and diffused into the polymer depends on the concentration and the temperature of the solution, and the period of the polymer treatment (Fig. 1, Curves 1 and 2, and Fig. 2, Curves 1–3).

With an increase in these parameters, the concentration of sulfur and selenium in the PA samples increases as well.

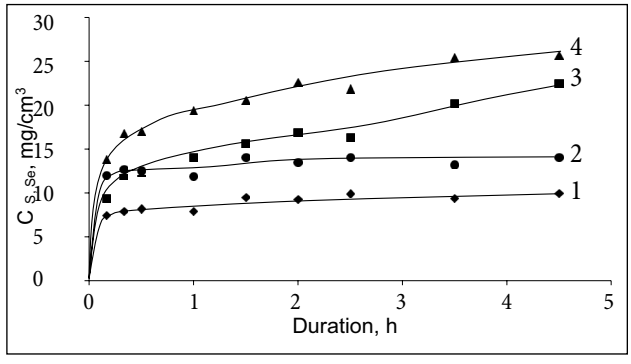

Fig. 1. Kinetics of sulfur (Curves 2 and 4) and selenium (Curves 1 and 3) sorption on PA at 50°C at different concentrations of precursor $K_2SeS_4O_6$ in 0.1 mol/dm^3 HCl: 1 and 2 – 0.025 mol/dm^3; 3 and 4 – 0.2 mol/dm^3

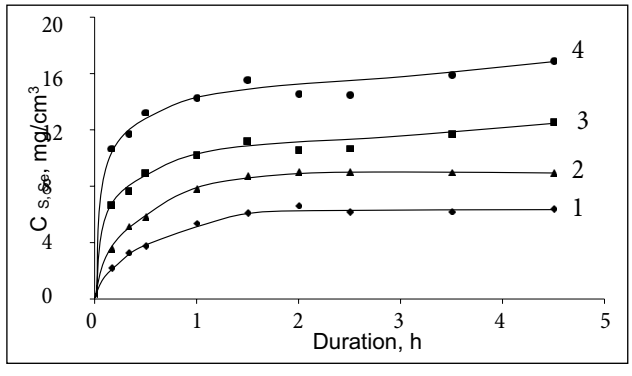

Fig. 2. Kinetics of sulfur (Curves 2 and 4) and selenium (Curves 1 and 3) sorption on PA treated with 0.05 mol/dm^3 solution of $K_2SeS_4O_6$ in 0.1 mol/dm^3 HCl at different temperatures °C: 1 and 2 – 30; 3 and 4 – 50

The maximal saturation of polymer with sulfur and selenium containing particles was reached in the PA samples seleniumized with a solution of higher concentration and temperature.

The $Cu_xSe–Cu_yS$ layers formed on the surface of PA samples when the chalcogeniumized PA samples were treated with the Cu(I/II) salt solution because of the heterogeneous redox reactions of selenopentathionate anions with Cu(I/II) solutions. Their colour of PA tapes became brown or even black, semiconductive or electrically conductive. The concentration of copper in the layer is strongly dependent on the concentrations of sulfur and selenium in PA, i.e. the concentration of copper increases with an increase of the sulfur and selenium concentrations in PA (Fig. 3). PA treated longer with $K_2SeS_4O_6$ requires more copper for the formation of a solid copper chalcogenide layer. A continuous chalcogenide layer decelerates a further increase of the copper concentration in the polymer. The concentration of copper in the chalcogenide layer on PA chalcogeniumized in selenopentathionate solutions changes uniformly only until the saturation has been reached (Fig. 3).

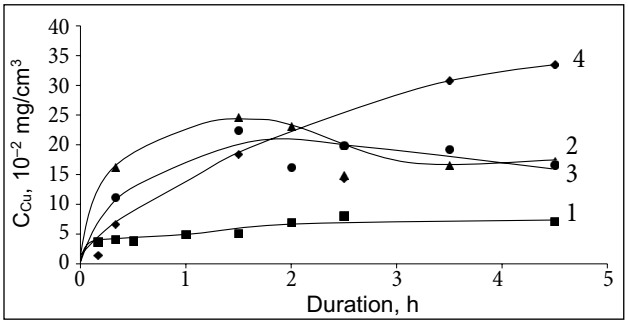

Fig. 3. Kinetics of the concentration of copper in the layer of copper chalcogenides on PA vs the time of initial PA treatment with $K_2SeS_4O_6$ solutions in 0.1 mol/dm^3 HCl at different temperatures: 1 – 0.025 mol/dm^3 at 50°C; 2 – 0.05 mol/dm^3 at 50°C; 3 – 0.2 mol/dm^3 at 50°C; 4 – 0.05 mol/dm^3 at 30°C

It was concluded that the concentration of copper is dependent on the conditions of the initial phase – on the concentration and temperature of precursor solution, and the duration of treatment.

The microscopic analysis of the PA surface, modified with copper chalcogenides, showed an irregular formation of $Cu_xSe–Cu_yS$ layers: they form islands. This unevenness increases the probability of the layer interactions with the impurities and cause some difficulties to the measurement of the surface electrical resistance. A detailed study of the resistance of PA modified with $Cu_xSe–Cu_yS$ layers was complicated, therefore we were satisfied to measure the electrical resistance of the chalcogenide surface outer layer only.

Under the conditions of experiments it was possible to form the layers of copper selenides–copper sulfides with the electrical sheet resistance varying from less than ~200 Ω/□ to even ~10 Ω/□ (Table).

The tendency of an electrical resistance decrease with an increase of the concentration of the precursor solution was observed. A direct dependence of the resistance of a chalcogenide layer on the concentration of copper in the layer was observed not in all cases, since copper chalcogenides of various stoichiometry and electrical conductivity and in different amounts may be formed. The increased number of phases and the intensity of its maxima reflect the increased concentration of copper sulfides and copper selenides on the surface of PA. The decrease of electrical resistance of these layers may be explained not only by the increase of copper chalcogenide phases concentration, but also by its qualitative changes, since it was known [32] that the electrical resistance of Cu_yS reduces by one million times while the value of y is reduced from 2 to 1. Because selenides are very close to sulfides the same standing rules apply to Cu_xSe.

Table. **Dependence of the electrical sheet resistance of copper chalcogenides layers on PA on the initial concentration of $K_2SeS_4O_6$ solution and the duration of chalcogeniumization at 50°C**

Duration, h	Electrical sheet resistance, Ω/□				
	The initial concentration of $K_2SeS_4O_6$, mol/dm^3 in 0.1 mol/dm^3 HCl				
	0.025	0.05	0.05*	0.1	0.2
0.5	178.0	88.0	145.8	48.6	60.0
1.0	99.7	70.4	84.5	71.0	32.7
1.5	72.0	63.8	54.3	48.0	19.8
2.0	68.7	61.7	44.2	52.5	14.4
2.5	61.5	51.8	47.9	47.0	13.6
3.5	53.6	42.9	42.8	32.5	12.3
4.5	18.8	60.5	42.7	20.8	13.0

* The temperature 30°C.

The X-ray diffraction patterns of the $Cu_xSe–Cu_yS$ films on the PA surface confirmed that peaks of various copper chalcogenide phases exist together in the layers.

XRD characterization

The phase composition of copper chalcogenides could be qualitatively and semi-quantitatively characterized by the X-ray diffraction. This method was successfully used in the number of cases to characterize the phase composition of copper chalcogenide layers in the surface of this polymer earlier [66, 68, 76–77]. Structural studies of the $Cu_xSe–Cu_yS$ layers were limited by the existence of copper chalcogenides phases with various compositions and structures, and by the crystallinity of the PA film itself. The intensities of its maximum at $2\theta < 25°$ exceeds the intensity of copper selenide at the maximum few times. Therefore the area of $2\theta \geq 25°$ was investigated in more detail.

The data received showed that the $Cu_xSe–Cu_yS$ layers formed indeed included several phases, and the composition varied with PA films chalcogeniumization conditions

and duration. All the peaks obtained are well matched with the Joint Committee on Powder Diffraction Standards (JCPDS). The XRD spectra of PA chalcogeniumized at different temperatures in the $K_2SeS_4O_6$ solutions of different concentration and different period of time showed peaks of various copper chalcogenide phases existing together in the film (Figs. 4, 5).

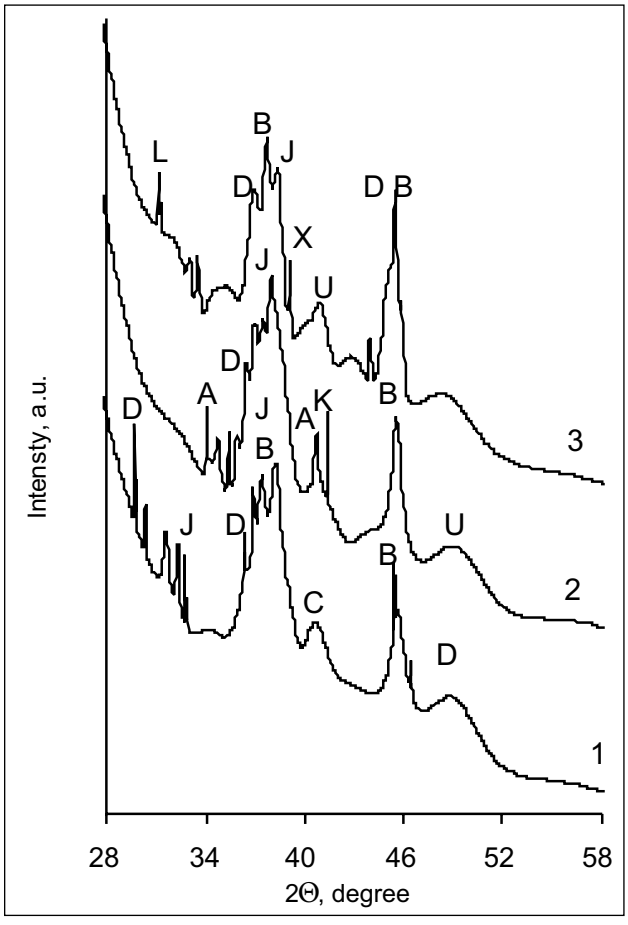

Fig. 4. X-ray diffraction patterns of the layers of chalcogenides on PA (peak of Cu_2S – C, $Cu_{1.9375}S$ – J, $Cu_{1.8}S$ – D, $Cu_{1.75}S$ – A, Cu_2Se – B, Cu_3Se_2 – U, CuSe – K, $CuSe_2$ – L, Cu_2Se_x – X) chalcogeniumized for 270 min at different temperature and then treated with Cu(II/I) salt solution: 1 – 0.05 mol/dm^3 at 30°C; 2 – 0.05 mol/dm^3 at 50°C; 3 – 0.2 mol/dm^3 at 50°C

The phases of *monoclinic djurleite*, $Cu_{1.9375}S$ (maxima at 2θ = 32.7 and 38.08°), *cubic digenite*, $Cu_{1.8}S$ (maxima at 2θ = 29.7, 36.3 and 49.1°), *orthorhombic chalcocite*, Cu_2S (maxima at 2θ = 40.9°), and *tetragonal bellidoite*, Cu_2Se (maxima at 2θ = 38.6 and 45.5°), were determined on the surface of PA chalcogeniumized at lower temperature (30°C). (Fig. 4, Curve 1).

On the surface of PA chalcogeniumized at higher temperature (50°C), besides the phases mentioned above, the phases of *orthorhombic anilite*, $Cu_{1.75}S$ (maxima at 2θ = 34.1 and 40.8°), *tetragonal umangite*, Cu_3Se_2 (maxima at 2θ = 49.2°), and *orthorhombic klockmannite*, CuSe (maxima at 2θ = 41.9°), were found, and the less conductive phase of *chalcocite*, Cu_2S, disappeared (Fig. 4, Curve 2).

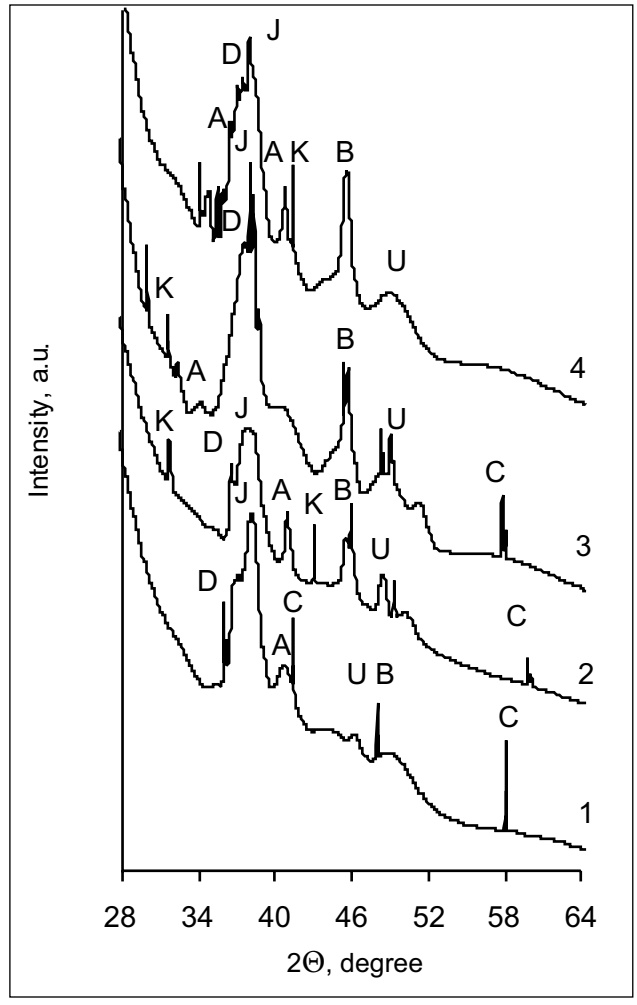

Fig. 5. X-ray diffraction patterns of the layers of chalcogenides on PA (peaks: Cu_2S – C, $Cu_{1.9375}S$ – J, $Cu_{1.8}S$ – D, $Cu_{1.75}S$ – A, Cu_2Se – B, Cu_3Se_2 – U, CuSe – K) treated first with 0.05 mol/dm^3 $K_2SeS_4O_6$ solution in 0.1 mol/dm^3 HCl at 50°C for different time and then with Cu(II/I) salt solution. The treatment time, min: 1 – 10; 2 – 60; 3 – 150; 4 – 270

With the increase of the concentration of precursor's solution the concentration of better conductive phases of $Cu_{1.9375}S$, $Cu_{1.8}S$ and of Cu_2Se increases and the phases of *anilite*, $Cu_{1.75}S$, and *klockmannite*, CuSe, disappear, but the new phases of *orthorhombic copper selenides*, $CuSe_2$ (maxima at 2θ = 31.4°) and Cu_2Se_x (maxima at 2θ = 39.1°), appear (Fig. 4, Curve 3).

The phase composition of Cu_xSe–Cu_yS layers with the increase of the duration of PA chalcogeniumization at the same temperature and concentration, remains almost unchanged but the concentration of less conductive *chalcocite* decreases and the concentration of electrically conductive copper sulphides and selenides increases (Fig. 5).

For example, only one new phase of *orthorhombic klockmannite*, CuSe, appears after 60 min (Fig. 5, Curve 2) and the less conductive phase of *chalcocite*, Cu_2S, dissapears (Fig. 5, Curve 4).

It was concluded that the increase of the concentration and temperature of precursor's solution and the duration of

PA treatment the highest concentration of conductive copper selenides are reached and the composition of Cu_yS phases changes in the direction of a decrease of y.

XPS characterization

XPS data (Fig. 6) showed a rather similar composition of Cu_xSe–Cu_yS layers formed in different experimental conditions. The presence of oxygen has been detected as the largest part (49–61 at.%) on the surface of all PA samples formed in ambient air. Therefore, the layers of chalcogenide on the surface of PA are distributed in the form of islands, that enable easy contacts of the atmospheric oxygen with ions of copper and chalcogens. The amount of oxygen significantly reduced (1–9 at.%) when the surface of the chalcogenide layer was etched by the Ar^+ ions.

That proves that oxygen is present on the surface of the chalcogenide layer only. The amount of O in the deeper layers is very small and its presence should not have any influence on the chemical composition of the layer and its properties. The oxygen in a deeper layer is undoubtly bound into the oxides Cu_2O and CuO. The presence of water connected by physical and chemical adsorption is also possible. For example, oxygen takes 56.89 at.% on the surface of PA chalcogeniumized in 0.05 mol/dm^3 $K_2SeS_4O_6$ solution during 10 min at 50°C.

A part of oxygen should be joined into the copper oxide, Cu_2O (bond energy E_b = 530.1 and 531.5 eV in the spectra of O 1*s*), and the value of E_b = 533.5 eV indicates the presence of the HO^- group. This group coud be from $Cu(OH)_2$, which probably forms by washing the chalcogenide layer with water. The presence of Cu(I) and Cu(II) sulfides in the surface of chalcogenide layers is indicated by E_b = 161.3 eV in the spectra of S 2*p*. The values of E_b = 53.8, 54.2, 55.3 eV in the spectra of Se 3*d* indicate the presence of elemental selenium. The spectra of Cu 2*p* confirmed the presence of the copper sulfides mentioned above and Cu_2O (E_b = 932.1 eV), and Cu(II) oxide, CuO (E_b = 933.9 eV).

The chemical composition of Cu_xSe–Cu_yS layers on the surface of PA initially chalcogeniumized for 1–4.5 h was similar to the same of layers formed with a shorter chalcogeniumization stage. The traces of elemental selenium were found in all samples studied since the solution of the precursor gradually decomposes with time.

When the chalcogenide layer was etched with Ar^+ ions, changes in the chemical composition and in the amounts of elements were detected. The amount of oxygen reduced by 6 times (to 9.38 at.%), but the amount of Cu, S and Se increased significantly. S 2*p* spectra indicated the formation of copper sulfides in the layer: the bond energy E_b = 161.5 eV showed the formation of Cu_2S, and E_b = 162.5 eV, respectively, CuS. The bond energy E_r = 932.2 eV in the spectra of Cu 2*p* confirmed the presence of copper sulfides and of Cu(I) oxide, Cu_2O, in the chalcogenide layer.

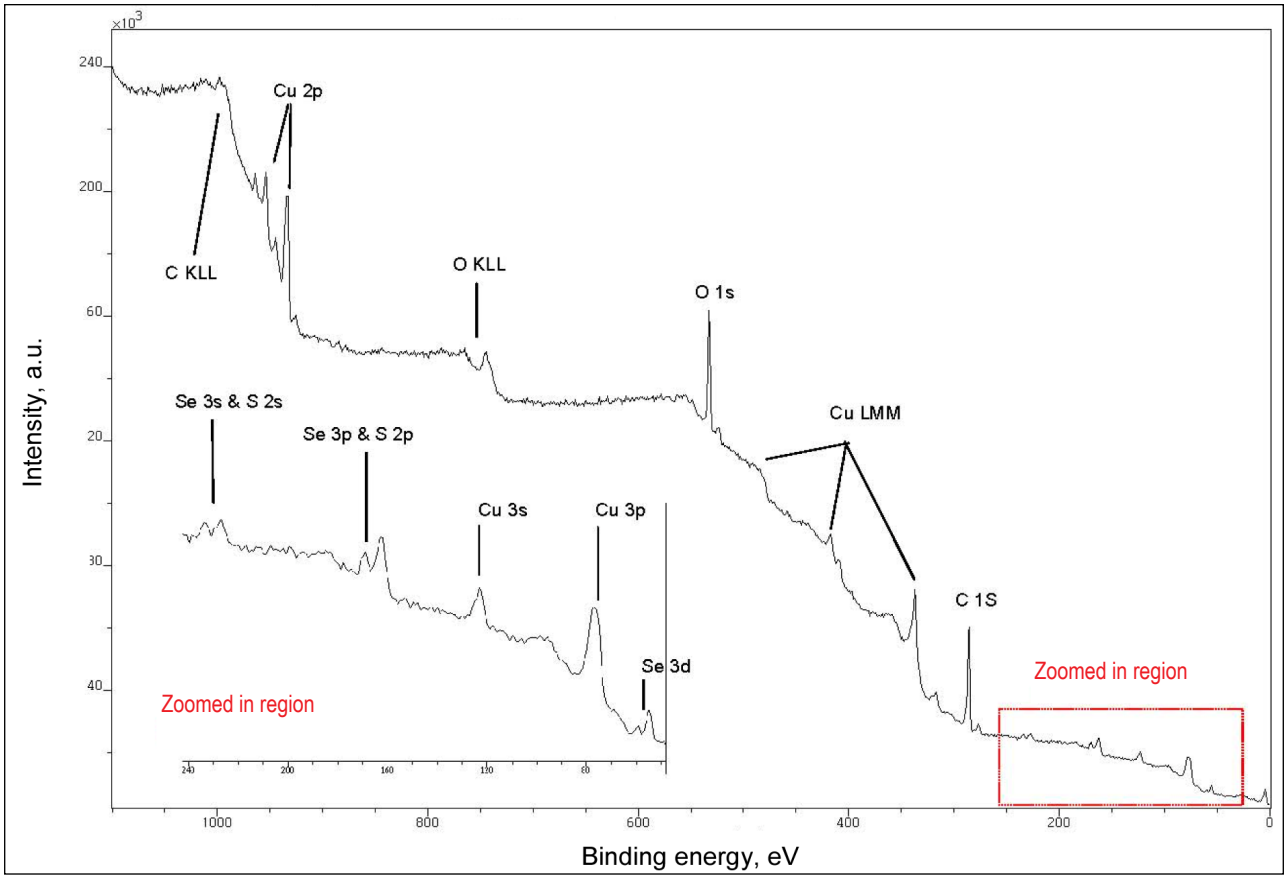

Fig. 6. XPS of the chalcogenide layers on PA treated first with 0.05 mol/dm^3 $K_2SeS_4O_6$ solution in 0.1 mol/dm^3 HCl and then with Cu(II/I) salt solution at 50°C

The morphology of $Cu_xSe–Cu_yS$ layers formed on the surface of PA

To characterize the morphology and to estimate the roughness of $Cu_xSe–Cu_yS$ layers, the method of atomic force microscopy was applied.

The morphological study of PA modified with $Cu_xSe–Cu_yS$ layers by atomic force microscopy revealed the coatings to be essentially different. Fields of 12 × 12 microns were investigated; for the quantitative estimation of the surface, the standard programs of the view treatment were used.

A view of the initial PA surface is presented in Fig. 7.

Views of the $Cu_xSe–Cu_yS$ layer surface obtained by AFM are shown in Figs. 8–11 and 14–15. The maximum height reaches ~67 nm, the average height (H_{mean}) ~28 nm; the root-mean square roughness is R_q 4.6 nm; the skewness is ~0.8.

It was determined that the height and surface morphology of the chalcogenide layers formed on PA depend on the conditions of polymer chalcogeniumization.

The profile sections of $Cu_xSe–Cu_yS$ coatings, presented below, allowed to estimate quantitatively the height and diameter of separate crystallites (Fig. 8, 11); the crystallinity of $Cu_xSe–Cu_yS$ layers was shown by X-ray diffraction [77].

When the polymer was chalcogenized at 30 °C, the height of the crystallites reached 478 nm (diameter ~0.1–2.0 μm) (Figs. 8, 9), the mean height being ~192 nm (Fig. 12).

On prolonging chalcogeniumization to 60 min, the height of crystallites changed insignificantly, decreased to 441 nm, and the diameter changed not much too and was equal to ~0.3–1.5 μm. The mean height of crystallites increased to ~217 nm, but after 270 min of chalcogenization the height of crystallites decreased to 338 nm (Fig. 11) (diameter ~0.3–2.1 μm), the H_{mean} of crystallites decreased ~1.4 times and equalled ~152 nm (Fig. 12).

Under a short duration of polymer treatment in the $K_2SeS_4O_6$ solution (10 min), the growth of the chalcogenide layer begins from the formation of separate small islands (Fig. 9). On prolonging chalcogenization to 60 min, the growth of the chalcogenide layer proceeds more intensively, and upon prolonging the duration of chalcogeniumization to 270 min, clusterization begins; as a result, the crystallites of various diameter and height begin slowly joining into agglomerates (Fig. 11).

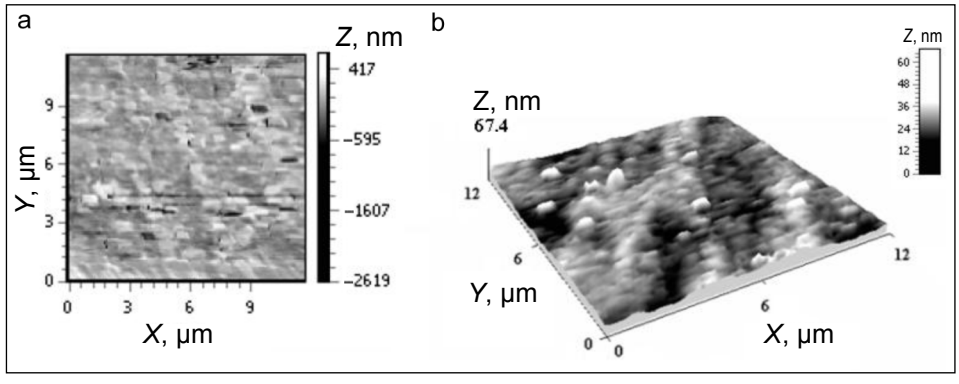

Fig. 7. An atomic force microscopy view of the initial (not chalcogeniumized) PA surface: a 2D view of lateral forces microscopy (a) and a 3D topography view (b). Scan field area 12 × 12 microns. The interval of unevenness height up to 67.4 nm

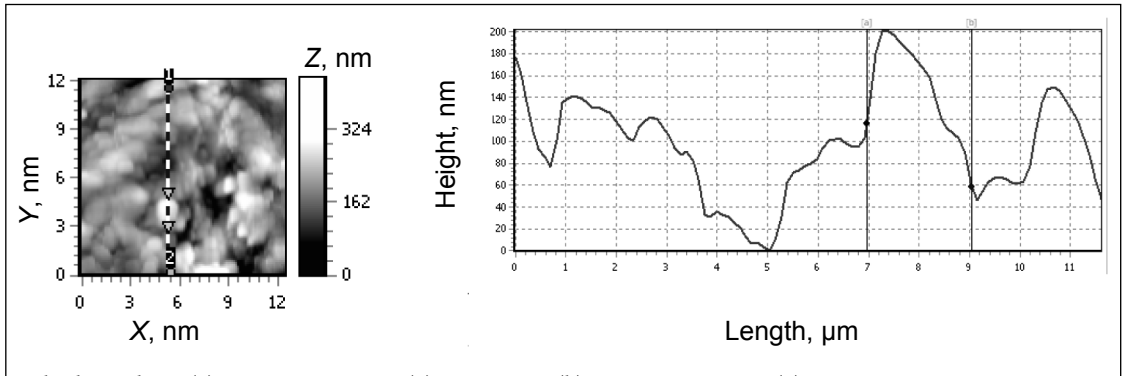

Absolute values : (a) → x = 6957.0 nm; $z(1)$ = 115.7 nm; (b) → x = 9054.8 nm; $z(1)$ = 57.7 nm;
Difference between markers: dx = 2097.8 nm; $dz(1)$ = 58.1 nm;
H_{mean} = 192.34 nm; R_a = 39.97; R_q = 50.52; R_{sk} = 0.06.

Fig. 8. A view of the topographic image and the line profile of the chalcogenide layer formed on the PA surface. PA was chalcogeniumized for 10 min at 30 °C in 0.05 mol/dm^3 $K_2SeS_4O_6$ solution and then treated with Cu(II/I) salts solution

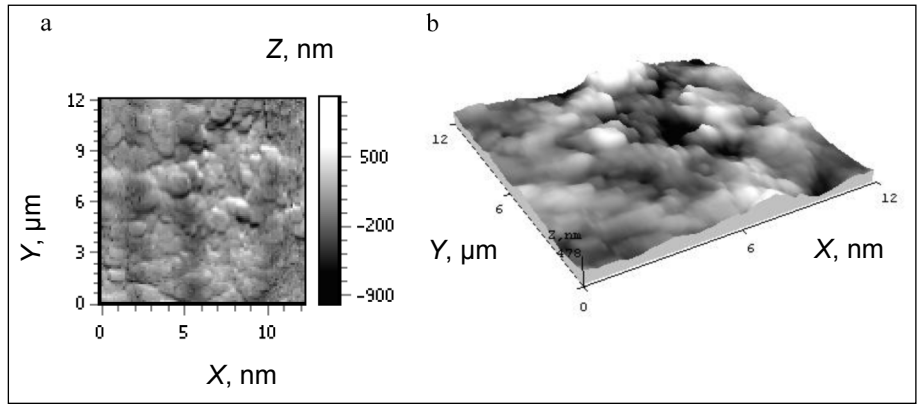

Fig. 9. An atomic force microscopy view of the $Cu_xSe–Cu_yS$ layers formed on the PA surface: a 2D view of lateral forces microscopy (a) and a 3D topography view (b). PA was chalcogenumized for 10 min at 30°C in 0.05 mol/dm^3 $K_2SeS_4O_6$ solution and then treated with Cu(II/I) salts solution

One can see a slight reduction of the mean layer roughness: from ~51 nm at the duration of chalcogeniumization of 10 min, to ~56 nm at the duration of 60 min and to ~36 nm at the duration of 270 min (Fig. 12). This means that the crystallites joining into agglomerates cover the surface more evenly, and the layer becomes more homogeneous.

Studying the formation of $Cu_xSe–Cu_yS$ layers on the PA surface, a chalcogenide layer was formed by changing the temperature also, i.e. PA was chalcogeniumized for 20, 60 and 270 min in the 0.05 mol/dm^3 $K_2SeS_4O_6$ solution at a temperature of 50°C and then treated with Cu(II/I) salt solution. The cross sections of these layers showed a rather uneven surface of the layers, the crystallites formed were of various height, diameter and shape.

When the polymer had been chalcogeniumized for 20–60 min at a temperature of 50°C, the maximum height of the layer decreased from 478–441 nm (chalcogeniumization duration 10 and 60 min at a temperature of 30°C) to ~348 nm, but the mean height of the layer decreased from ~192–217 nm to ~107–129 nm. On prolonging chalcogeniumization to 270 min and at the same conditions of "copperizing", the H_{mean} of crystallites increased from ~152 nm (at 30°C) to ~296 nm (at 50°C, Fig. 13). The same tendency was observed in a change of the $Cu_xSe–Cu_yS$ layer roughness increasing the chalcogeniumization temperature from 30 to 50°C: it increased from ~36 nm to ~83 nm (Fig. 13).

Thus, with increasing the chalcogeniumization temperature from 30 to 50°C depending on time, the height and roughness of crystallites change. The reason may be the differences in the phase composition of $Cu_xSe–Cu_yS$ layers obtained at a different temperature: that was shown in the previous study [77] on the X-ray diffraction investigation of $Cu_xSe–Cu_yS$ layers formed on the PA film surface.

Copper chalcogenide layers were formed using PA chalcogeniumization in 0.2 mol/dm^3 $K_2SeS_4O_6$ solution for 20, 60 and 270 min at a temperature of 50°C. The views of the layers formed are shown in Figs. 14 and 15.

On increasing the duration of PA chalcogeniumization from 60 to 270 min, the number of islands increased, some of them joined into large agglomerates formed of crystallites of

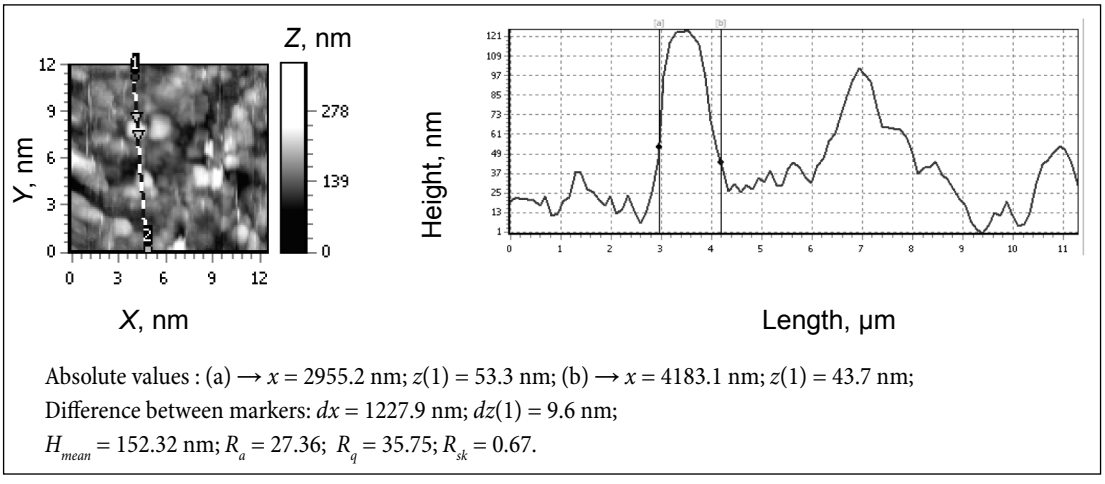

Fig. 10. A view of the topographic image and the line profile of the chalcogenide layer formed on the PA surface. PA was chalcogeniumized for 270 min at 30°C in 0.05 mol/dm^3 $K_2SeS_4O_6$ solution and then treated with Cu(II/I) salts solution

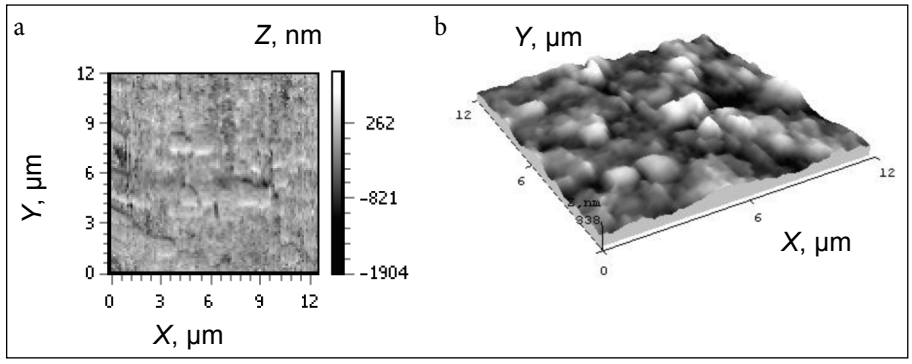

Fig. 11. An atomic force microscopy view of the $Cu_xSe–Cu_yS$ layers formed on the PA surface: a 2D view of lateral forces microscopy (a) and a 3D topography view (b). PA was chalcogeniumized for 270 min at 30°C in 0.05 mol/dm^3 $K_2SeS_4O_6$ solution and then treated with Cu(II/I) salts solution

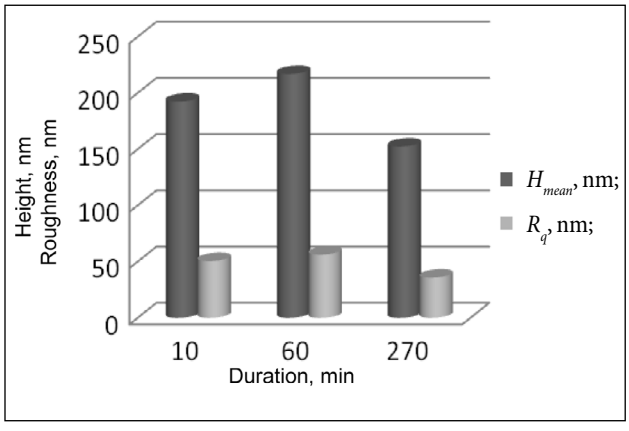

Fig. 12. Dependence of the layer mean square roughness and the mean height on the duration of PA treatment in 0.05 mol/dm^3 $K_2SeS_4O_6$ solution at a temperature of 30°C

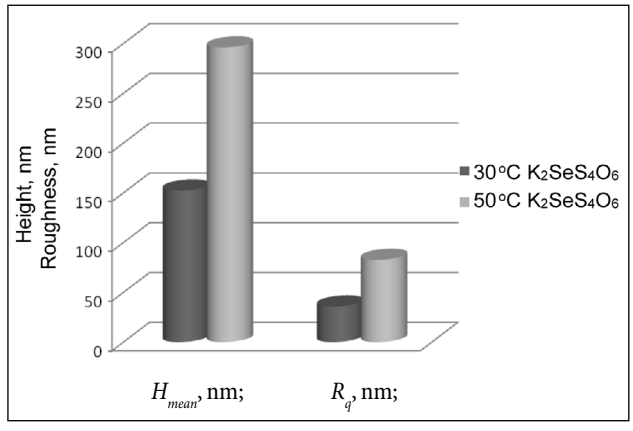

Fig. 13. Dependence of the $Cu_xSe–Cu_yS$ layer mean height (H_{mean}) and the root mean square roughness (R_q) on the temperature of 0.05 mol/dm^3 $K_2SeS_4O_6$ solution while treating PA during 270 min

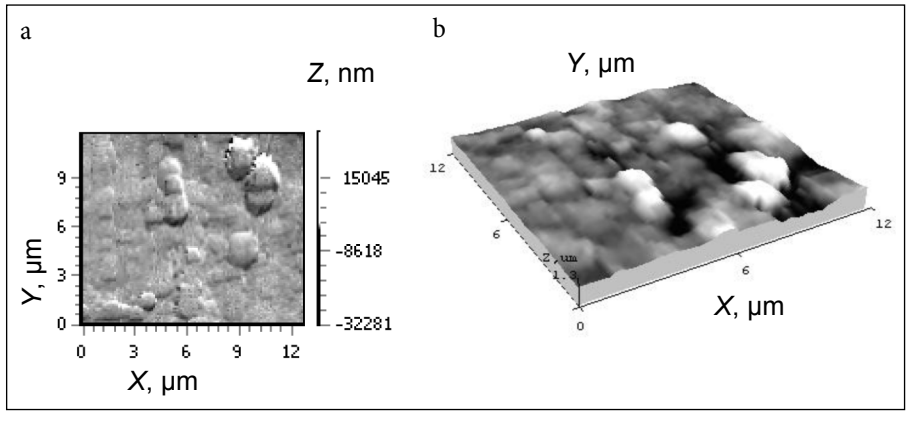

Fig. 14. An atomic force microscopy view of the CuxSe–CuyS layers formed on the PA surface: a 2D view of lateral forces microscopy (a) and a 3D topography view (b). PA was chalcogenized for 60 min at 50°C in 0.2 mol/dm^3 $K_2SeS_4O_6$ solution and then treated with Cu(II/I) salts solution

different diameter; the maximum height of the layer increasing the chalcogeniumization duration increased from ~1000 to ~1300 nm and the roughness of the layer increased from ~99 to ~112 nm (Figs. 14, 15).

Comparing the results of the $Cu_xSe–Cu_yS$ layers morphological characteristics (Fig. 16), received using 0.05 and 0.2 mol/dm^3 $K_2SeS_4O_6$ solutions at a temperature of 50°C (duration of chalcogeniumization 60 min), it was concluded that

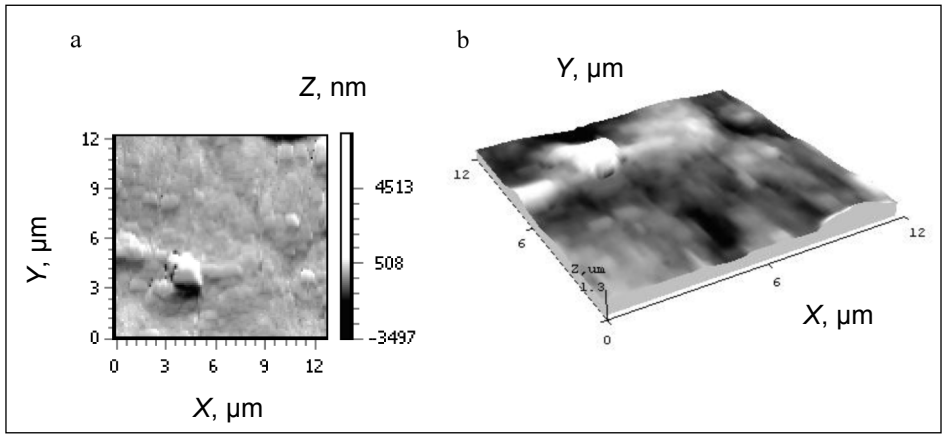

Fig. 15. An atomic force microscopy view of the $Cu_xSe–Cu_yS$ layers formed on the PA surface: a 2D view of lateral forces microscopy (a) and a 3D topography view (b). PA was chalcogenized for 270 min

the copper chalcogenide layer mean height (from ~107 to ~1000 nm) and the root mean square roughness (from ~31 to ~99 nm) increased with an increase of the chalcogeniumization solution concentration.

But as it is seen in Figs. 14 and 15, separate islands join into large agglomerates and almost evenly cover the surface of polyamide (Fig. 15).

Thus, the AFM results indicate that depending on the conditions (duration of chalcogeniumization, concentration and temperature) of PA initial chalcogeniumization in the $K_2SeS_4O_6$ solution (under the same "copperizing" conditions), the formation of copper chalcogenide layers proceeds irregularly in the form of islands which grow into larger agglomerates. The surface of the layer is uneven, rather rough.

The results presented above showed that when for a polyamide chalcogeniumization 0.05–0.2 mol/dm^3 $K_2SeS_4O_6$ solutions were used, the highest concentration of conductive copper selenides and copper sulfides was reached in the case of 0.2 mol/dm^3 solution of $K_2SeS_4O_6$. As a result, very low values of the electrical sheet resistance (up to ~12 Ω/□) of chalcogenide layers on PA were formed (The concept of sheet resistance is used to characterize thin deposited layers. Sheet resistance is specified by the unit "ohms per square", Ω/□, ohms/square). This data of earlier studies are in agreement with the results of the morphology study, presented here: the separate crystallites, increasing the duration of PA chalcogeniumization, join into larger agglomerates, which more evenly cover the surface of polyamide; when the $Cu_xSe–Cu_yS$ layer becomes homogeneous, its electrical resistance reaches the lowest values.

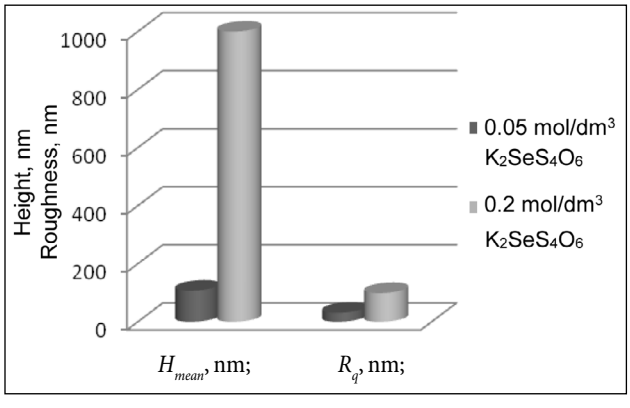

Fig. 16. Dependence of the $Cu_xSe–Cu_yS$ layers mean height (Hmean) and the root mean square roughness (R_q) on the concentration of 50°C $K_2SeS_4O_6$ solution while treating PA during 60 min

Received 20 June 2017
Accepted 26 September 2017

References

1. Ch. Ma, D. Moore, Y. Ding, J. Li, Z. L. Wang, *Int. J. Nanotechnology*, **1(4)**, 431 (2004).
2. M. T. S. Nair, P. K. Nair, *Semicond. Sci. Technol.*, **4**, 191 (1989).
3. P. M. Keane, H. F. Franzen, in: R. Bruce King (ed.), *Encyclopedia of Inorganic Chemistry*, Vol. 7, 610, John Wiley & Sons, Chichester, New York, Brisbane, Toronto, Singapore (1994).
4. S. Dhar, S. Chakrabarti, *J. Appl. Phys.*, **82(2)**, 655 (1997).
5. R. Blachnik, A. Müller, *Thermochim. Acta*, **361(1–2)**, 31 (2000).
6. X. Jiang, Y. Xie, J. Lu, W. He, L. Zhu, Y. Qian, *J. Mater. Chem.*, **10**, 2193 (2000).
7. Z. Nan, X. Y. Wang, Z. Zhao, *J. Cryst. Growth*, **295(1)**, 92 (2006).
8. G. She, X. Zhang, W. Shi, et al., *Cryst. Growth Des.*, **8(6)**, 1789 (2008).
9. H. Anders, G. Michael, *Chem. Rev.*, **95(1)**, 49 (1995).
10. W. Z. Wang, Y. Geng, P. Yan, F. Y. Liu, Y. Xie, Y. T. Qian, *J. Am. Chem. Soc.*, **121(16)**, 4062 (1999).
11. W. S. Chen, J. M. Stewart, R. A. Mickelsen, *Appl. Phys. Lett.*, **46(11)**, 1095 (1985).

12. C. Nascu, I. Pop, V. Ionescu, E. Indrea, I. Bratu, *Mater. Lett*., **32(2–3)**, 73 (1997).
13. H. Okimura, R. Matsumae, R. Makabe, *Thin Solid Films*, **71(1)**, 53 (1980).
14. M. A. Korzhuev, *Phys. Solid State*, **40(2)**, 217 (1998).
15. P. K. Nair, V. M. Garcia, A. M. Fernandez, H. S. Ruiz, M. T. S. Nair, *J. Phys. D: Appl. Phys.*, **24(3)**, 441 (1991).
16. J. Cardoso, O. Gomez-Daza, L. Ixtlilco, M. T. S. Nair, P. K. Nair, *Semicond. Sci. Technol*, **16(2)**, 123 (2001).
17. V. M. Garcia, P. K. Nair, M. T. S. Nair, *J. Cryst. Growth*, **203(1–2)**, 113 (1999).
18. A. Galdikas, A. Mironas, V. Strazdienė, A. Šetkus, I. Ancutienė, V. Janickis, *Sens. Actuators B*, *Chem.*, **67**, 76 (2000).
19. A. Šetkus, A. Galdikas, A. Mironas, et al., *Thin Solid Films*, **391**, 275 (2001).
20. A. Šetkus, A. Galdikas, A. Mironas, et al., *Sens. Actuators B, Chem.*, **78**, 208 (2001).
21. L. Ancutienė, V. Janickis, R. Ivanauskas, A. J. Galdikas, A. Mironas, A. Šetkus, V. Strazdienė, Lithuanian Patent LT 4584 B, 1999.
22. R. Maciulevičius, V. Janickis, R. Ivanauskas, Lithuanian Patent LT 4402 B, 1998.
23. R. Ivanauskas, V. Janickis, V. Zelionkaitė, A. Žebrauskas, Lithuanian Patent LT 4235 B, 1997.
24. I. Ancutienė, V. Janickis, A. J. Galdikas, A. Mironas, A. Šetkus, V. Strazdienė, I. Šimkienė, Lithuanian Patent LT 4802 B, 2001.
25. I. Ancutienė, V. Janickis, A. J. Galdikas, A. Mironas, A. Šetkus, V. Strazdienė, I. Šimkienė, Lithuanian Patent LT 4805 B, 2001.
26. V. Janickis, R. Ivanauskas, A. E. Ancuta, N. Petrašauskienė, Lithuanian Patent LT 5119 B, 2004.
27. V. Janickis, R. Ivanauskas, I. Ancutienė, V. J. Šukytė, N. Petrašauskienė, Lithuanian Patent LT 5266 B, 2005.
28. J. Zhou, X. Wu, A. Duda, G. Teeter, *Thin Solid Films*, **515(18)**, 7364 (2007).
29. X. Wu, J. Zhou, A. Duda, et al., Thin Solid Films, **515(15)**, 5798 (2007).
30. N. Petrašauskienė, V. Janickis, R. Ivanauskas, *Chem. Technol.*, **2(32)**, 10 (2004).
31. M. Öztaş, M. Bedir, A. N. Yazici, E. V. Kafadar, H. Toktamış, *Phys. B*, **381(1–2)**, 40 (2006).
32. A. Žebrauskas, *Chem. Technol.*, **1(3)**, 39 (1996).
33. S. Lindroos, A. Arnold, M. Leskela, *Appl. Surf. Sci.*, **158(1–2)**, 75 (2000).
34. S. D. Sartale, C. D. Lokhande, *Mater. Chem. Phys.*, **65(1)**, 63 (2000).
35. E. Fatas, T. Garcia, C. Montemayor, A. Medina, E. Garcia Camarero, F. Arjona, *Mater. Chem. Phys.*, **12(2)**, 121 (1985).
36. R. S. Mane, C. D. Lokhande, *Mater. Chem. Phys.*, **65(1)**, 1 (2000).
37. R. Ivanauskas, V. Janickis, R. Maciulevičius, *Chem. Technol.*, **4(13)**, 71 (1999).
38. R. Maciulevičius, V. Janickis, R. Ivanauskas, *Chemija*, **11(4)**, 141 (2000).
39. R. Ivanauskas, R. Rumša, V. Janickis, *Chem. Technol.*, **3(20)**, 47 (2001).
40. R. Ivanauskas, R. Rumša, V. Janickis, A. Baltušnikas, *Chem. Technol.*, **4(25)**, 60 (2002).
41. V. Krylova, R. Ivanauskas, V. Janickis, *Chem. Technol.*, **4(25)**, 56 (2002) [in Lithuanian].
42. V. Janickis, R. Maciulevičius, R. Ivanauskas, I. Ancutienė, *Colloid Polym. Sci.*, **281**, 84 (2003).
43. V. Janickis, R. Maciulevičius, R. Ivanauskas, *Mater. Sci. (Medžiagotyra)*, **10(3)**, 225 (2004).
44. V. Janickis, R. Maciulevicius, R. Ivanauskas, I. Ancutiene, *Mater. Sci.-Poland*, **23(3)**, 715 (2005).
45. R. Ivanauskas, R. Stokienė, V. Janickis, N. Kreivėnienė, *Chem. Technol.*, **1(35)**, 20 (2005).
46. V. Janickis, R. Ivanauskas, R. Stokienė, N. Kreivėnienė, *Chem. Technol.*, **3(37)**, 32 (2005).
47. V. Janickis, R. Stokienė, R. Ivanauskas, N. Kreivėnienė, *Chemija*, **17(4)**, 7 (2006).
48. R. Ivanauskas, V. Janickis, R. Stokienė, *Chem. Technol.*, **1(39)**, 29 (2006).
49. I. Ancutiene, V. Janickis, R. Ivanauskas, *Appl. Surf. Sci.*, **252(12)**, 4218 (2006).
50. V. Janickis, G. Usonytė, N. Kreivėnienė, *Chem. Technol.*, **2(44)**, 47 (2007).
51. G. Usonytė, V. Janickis, N. Kreivėnienė, *Chem. Technol.*, **3(45)**, 31 (2007).
52. I. Ancutiene, V. Janickis, R. Ivanauskas, R. Stokiene, N. Kreiveniene, *Polish J. Chem.*, **81**, 381 (2007).
53. V. Janickis, R. Ivanauskas, R. Stokienė, *Chemija*, **19(1)**, 32 (2008).
54. G. Usonytė, V. Janickis, N. Kreivėnienė, *Mater. Sci. (Medžiagotyra)*, **14(1)**, 34 (2008).
55. V. Janickis, R. Ivanauskas, R. Stokienė, M. Andrulevičius, *Chemija*, **20(1)**, 45 (2009).
56. I. Ancutienė, V. Janickis, R. Stokienė, *Chemija*, **20(1)**, 38 (2009).
57. R. Stokienė, V. Janickis, *Chem. Technol.*, **4(53)**, 33 (2009).
58. R. Ivanauskas, V. Janickis, I. Ancutienė, R. Stokienė, *Cent. Eur. J. Chem.*, **7(4)**, 864 (2009).
59. V. Janickis, R. Stokienė, *Chemija*, **21(1)**, 33 (2010).
60. R. Ivanauskas, V. Janickis, *Chemija*, **1**, 3 (1998).
61. R. Ivanauskas, V. Janickis, *Ukr. Khim. Zh.*, **65(5)**, 49 (1999).
62. R. Ivanauskas, V. Janickis, *Prog. Colloid Polym. Sci.*, **116**, 134 (2000).
63. R. Ivanauskas, V. Janickis, S. Žalenkienė, V. Jasulaitienė, *Chem. Technol.*, **1(39)**, 34 (2006).
64. R. Ivanauskas, V. Janickis, *Polish J. Chem.*, **82**, 2281 (2008).
65. V. Janickis, R. Ivanauskas, N. Petrašauskienė, *Chem. Technol.*, **3(16)**, 23 (2000).
66. R. Ivanauskas, V. Janickis, N. Petrašauskienė, *Mater. Sci. (Medžiagotyra)*, **6(4)**, 298 (2000).
67. N. Petrašauskienė, R. Ivanauskas, V. Janickis, *Chem. Technol.*, **1(27)**, 32 (2003).
68. V. Janickis, R. Ivanauskas, N. Petrašauskienė, *Chem. Technol.*, **2(28)**, 17 (2003).
69. R. Ivanauskas, J. Šukytė, V. Janickis, N. Petrašauskienė, *Mater. Sci. (Medžiagotyra)*, **10(1)**, 29 (2004).

70. N. Petrašauskienė, R. Ivanauskas, V. Janickis, R. Stokienė, V. Jasulaitienė, *Chem. Technol.*, **4(34)**, 24 (2004).
71. N. Petrašauskienė, A. Žebrauskas, V. Janickis, R. Ivanauskas, *Chemija*, **15(4)**, 1 (2004).
72. J. Šukytė, R. Ivanauskas, N. Petrašauskienė, V. Janickis, S. Žalenkienė, *Chem. Technol.*, **2(36)**, 46 (2005).
73. J. Šukytė, R. Ivanauskas, N. Petrašauskienė, V. Janickis, *Proceedings of the 8th International Conference on Solar Energy and Applied Photochemistry [SOLAR'05]. The 5th International Workshop on Environmental Photochemistry [ENPHO'06]*, Cairo, Egypt (2005).
74. V. Janickis, R. Ivanauskas, N. Petrašauskienė, J. Šukytė, *NanoTech Insight 2005: International Conference on Nanotechnology: Program and Abstracts*, Luxor, Egypt (2005).
75. V. Janickis, N. Petrašauskienė, R. Ivanauskas, *Mater. Sci. (Medžiagotyra)*, **11(2)**, 110 (2005).
76. N. Petrašauskienė, V. Janickis, *Chemija*, **20(1)**, 56 (2009).
77. N. Petrašauskienė, V. Janickis, V. Šukytė, *Polish J. Chem.*, **83(3)**, 401 (2009).
78. V. Janickis, *Polythionates*, Monography, Technology, Kaunas (2006).
79. V. Janickis, *Seleno- and Telluropolythionates*, Monography, Technology, Kaunas (2007).
80. N. Petrašauskienė, V. Janickis, *Chemija*, **22(1)**, 25 (2011).
81. N. Petrašauskienė, R. Stokienė, S. Žalenkienė, V. Janickis, *Chemija*, **26**(2), 93 (2015).
82. N. Petrašauskienė, S. Žalenkienė, V. Janickis, V. Jasulaitienė, R. Stokienė, *Mater. Sci. (Medžiagotyra)*, **21(1)**, 7 (2015).
83. O. Foss, in: H. J. Emeleus, A. G. Sharpe (eds.), *Advances in Inorganic Chemistry and Radiochemistry*, Vol. 2, 237, Academic Press, New York (1960).
84. A. Žebrauskas, A. Mikalauskienė, V. Latvys, *Chemistry*, **3**, 131 (1992) [in Russian].
85. I. Ancutienė, V. Janickis, S. Grevys, *Chemistry*, **3**, 3 (1997).
86. O. Foss, *Acta Chem. Scand.*, **3**, 435 (1949).
87. *Analytical Methods for Atomic Absorption Spectrometry*, Perkin Elmer Corporation (1973).
88. A. J. Vogel, *Text Book of Quantitative Chemical Analysis*, 5th edn., Longman Scientific & Technical, London (1989).
89. D. Briggs, in: M. P. Seach (ed.), *Practical Surface Analysis by Auger and X-ray Photoelectron Spectroscopy*, John Wiley and Sons, Chichester (1983).
90. C. D. Wagner, W. M. Riggs, L. E. Davis, J. F. Moulder, *Handbook of X-Ray Photoelectron Spectroscopy*, Perkin-Elmer Corporation, Minnesota (1978).

Vitalijus Janickis, Neringa Petrašauskienė

POLIAMIDO PLĖVELIŲ MODIFIKAVIMAS PUSLAIDŽIAIS IR LAIDŽIAIS VARIO SELENIDŲ-VARIO SULFIDŲ SLUOKSNIAIS

S a n t r a u k a

Poliamido 6 (PA) plėvelių paviršiaus modifikavimas puslaidžiais ir laidžiais mišriųjų vario selenidų-vario sulfidų Cu_xSe-Cu_yS sluoksniais atliktas mūsų ištobulintu sorbciniu-difuziniu metodu ir vandeniniais kalio selenopentationato $K_2SeS_4O_6$ tirpalais, kaip polimero chalkogeninimo pirmtakais. Selenopentationato anijonai ^-O_3S-S-Se-S-SO_3^-, turintys dvivalenčius, žemo oksidacijos laipsnio seleno ir sieros atomus, sorbuoja-difunduoja į PA plėveles, jei jos apdorojamos selenopentationato tirpalais. Cu_xSe–Cu_yS sluoksniai PA plėvelių paviršiuje susidaro tada, kai chalkogenintas polimeras apdorojamas vandeniniu vario(II/I) druskų tirpalu: selenopentationato anijonai reaguoja su vario jonais. Sieros, seleno ir vario koncentracijos chalkogenidų sluoksniuose auga didėjant pradinio PA chalkogeninimo pirmtako tirpalo koncentracijai, temperatūrai ir chalkogeninimo trukmei. Susidarę sluoksniai charakterizuoti chemine sudėtimi, elektrinėmis ir fizinėmis savybėmis. Kiekybiniai seleno, sieros ir vario kiekiai Cu_xSe–Cu_yS sluoksniuose PA plėvelių paviršiuje didėja ilgėjant polimero chalkogeninimo trukmei. Rentgeno struktūriniai Cu_xSe–Cu_yS sluoksnių tyrimai parodė, kad jie yra polikristaliniai. Identifikuotos šešios vario selenidų Cu_2Se, $CuSe_2$, $CuSe_2$, Cu_3Se_2 ir berzelianito $Cu_{2-x}Se$ bei bellidoito Cu_2Se, taip pat keturios vario sulfidų – monoklininio djurleito $Cu_{1,9375}Se$, kubinio digenito $Cu_{1,8}S$, ortorombinio chalkocito Cu_2S ir ortorombinio anilito $Cu_{1,75}S$ fazės.

Didėjant pirmtako tirpalo koncentracijai, temperatūrai ir PA apdorojimo trukmei, pasiekiama didžiausia laidžių elektrai vario selenidų koncentracija, o Cu_xS fazių sudėtis kinta x vertės mažėjimo kryptimi. Tyrimų rentgeno difrakcinės spektrinės analizės metodu gauti rezultatai patvirtino vario selenidų-vario sulfidų sluoksnių PA paviršiuje susidarymą. Nustatyti dėsningumai įgalina norimos sudėties ir laidžio elektrai Cu_xSe–Cu_yS sluoksnių susidarymą. Tyrimai atominių jėgų mikroskopijos metodu parodė, kad priklausomai nuo PA pradinio halkogeninimo $K_2SeS_4O_6$ tirpale sąlygų (trukmės, koncentracijos ir temperatūros), esant toms pačioms „variavimo" sąlygoms, chalkogenidų sluoksnių susidarymas vyksta netolygiai salelių pavidalu, kurios auga į didesnius aglomeratus. Sluoksnio paviršius yra netolygus ir gana šiurkštus.